Atmospheric Gas-Phase Reactions of Selected Phosphorus-Containing Compounds

Pilar Martin,[†] Ernesto C. Tuazon,* Roger Atkinson,*[,‡] and A. David Maughan[§]

Air Pollution Research Center, University of California, Riverside, California 92521

Received: July 16, 2001

The kinetics of the gas-phase reactions of phosphorus oxychloride [$P(O)Cl_3$], methylphosphonic dichloride [$CH_3P(O)Cl_2$], dimethyl phosphonate [$(CH_3O)_2P(O)H$], and trimethyl phosphite [$(CH_3O)_3P$] with the OH radical were measured at 298 ± 2 K and 1 atm (~740 Torr) of dry air by a relative rate method which employed the photolysis of CH_3ONO as the source of OH radicals and analysis of the reaction mixtures by in-situ Fourier transform infrared (FT-IR) spectroscopy. The measured values of the OH radical reaction rate constants (cm^3 $molecule^{-1}$ s^{-1}) are the following: $P(O)Cl_3$, $< 4 \times 10^{-14}$; $CH_3P(O)Cl_2$, $(6.4 \pm 2.1) \times 10^{-14}$; $(CH_3O)_2P(O)H$, $(5.08 \pm 0.53) \times 10^{-12}$; and $(CH_3O)_3P$, $(7.1 \pm 0.9) \times 10^{-10}$, corresponding to estimated tropospheric lifetimes of >290 days, 180 days, 2.3 days, and 0.016 day, respectively, for the reactions of these compounds with OH radicals. In support of the OH radical rate constant measurement for $(CH_3O)_3P$, the absolute rate constant for the $NO_2 + (CH_3O)_3P$ reaction was measured and determined to be $(3.8 \pm 0.4) \times 10^{-18}$ cm^3 $molecule^{-1}$ s^{-1} at 298 ± 2 K. The products of the reaction of dimethyl phosphonate with the OH radical and those of trimethyl phosphite with the OH radical, NO_2, and O_3 were investigated by FT-IR spectroscopy and atmospheric pressure ionization mass spectrometry (API-MS).

Introduction

Phosphorus-containing compounds such as alkyl and/or aryl phosphates [$(RO)_3PO$] and alkylphosphonates [$(RO)_2P(O)R$], where R = aryl, alkyl, or H, are used as plasticizers, flame retardants, and fire-resistant fluids and lubricants, and organophosphorus compounds of the structure $(RO)_3PO$ and $(RO)_3PS$ are widely used as pesticides.[1] The manufacture of these and other organophosphorus compounds employs inorganic and organic phosphorus intermediates such as PCl_3, $P(O)Cl_3$, $RP(O)X_2$, $RP(S)X_2$, $(RO)_aP(O)X_{3-a}$, and $(RO)_aP(S)X_{3-a}$, where R = alkyl, X = halogen, and $a = 1$ or 2.[1] The use of phosphorus-containing compounds as intermediates or end-products results in their release into the atmosphere, either intentionally in the case of pesticide application or inadvertently in the case of chemical intermediates and flame retardants, etc., where they can react and undergo transport.

In the atmosphere, organic compounds present in the gas phase can undergo photolysis (at wavelengths >290 nm in the troposphere); reactions with OH radicals, NO_3 radicals, and O_3; and wet and dry deposition (the later processes also being important for particle-associated chemicals).[2] To date, there are relatively few data available concerning the atmospheric chemistry of phosphorus-containing compounds. Rate constants for the potentially atmospherically important reactions of the OH radical with the inorganic compounds phosphine,[3] phosphorus tribromide,[4] and phosphorus trichloride[5] have been measured, and rate constants for the reactions of OH and NO_3 radicals and O_3 with the organophosphorus compounds $(CH_3O)_3PO$,[6] $(C_2H_5O)_3PO$,[7] $(CH_3O)_2P(S)Cl$,[7] $(CH_3O)_3PS$,[8] $(CH_3O)_2P(S)SCH_3$,[8] $(CH_3O)_2P(O)SCH_3$,[8] $(CH_3S)_2P(O)OCH_3$,[8] $(CH_3O)_2P(O)N(CH_3)_2$,[9] $(CH_3O)_2P(S)N(CH_3)_2$,[9] $(CH_3O)_2P(S)NHCH_3$,[9] and $(CH_3O)_2P(S)NH_2$[9] have been reported.

In this work, we have measured rate constants for the reactions of OH radicals with the four phosphorus-containing compounds phosphorus oxychloride [$P(O)Cl_3$]; methylphosphonic dichloride [$CH_3P(O)Cl_2$]; dimethyl phosphonate [$(CH_3O)_2P(O)H$], also called dimethyl phosphite; and trimethyl phosphite [$(CH_3O)_3P$]. These compounds are either used as intermediates in the manufacture of other phosphorus-containing compounds and/or are representatives of classes of organophosphorus compounds for which no rate constant data are presently available. The products of the reaction of dimethyl phosphonate with OH radicals and of trimethyl phosphite with OH radicals, NO_2, and O_3 were also investigated.

Experimental Section

Kinetic Studies. Rate constants for the gas-phase reactions of the hydroxyl radical with the four selected phosphorus-containing compounds (hereafter denoted P-compounds) were measured using a relative rate technique, in which the relative disappearance rates of the P-compound and a reference compound, whose OH radical reaction rate constant is reliably known, were measured in the presence of OH radicals. Under these conditions,

$$\ln([P]_{t_0}/[P]_t) = (k_1/k_2) \ln([R]_{t_0}/[R]_t) \quad \text{(I)}$$

where $[P]_{t_0}$ and $[R]_{t_0}$ are the concentrations of the P-compound and the reference compound, respectively, at time t_0, $[P]_t$ and $[R]_t$ are the corresponding concentrations at time t, and k_1 and k_2 are the rate constants for reactions 1 and 2, respectively.

$$OH + P \rightarrow \text{products} \quad (1)$$

$$OH + R \rightarrow \text{products} \quad (2)$$

* Authors to whom correspondence should be addressed. Phone: 909-787-5140. Fax: 909-787-5004. E-mail: ernesto.tuazon@ucr.edu.

[†] Present Address: Universidad de Castilla-La Mancha, Facultad de Ciencias, Campus Universitario s/n, 13071, Ciudad Real, Spain.

[‡] Also, Interdepartmental Graduate Program in Environmental Toxicology, Department of Environmental Sciences, and Department of Chemistry.

[§] Pacific Northwest National Laboratory, 902 Battelle Boulevard, P.O. Box 999, Richland, WA 99352.

10.1021/jp012720d CCC: $22.00
Published on Web 02/02/2002

Hence, a plot of $\ln([P]_{t_0}/[P]_t)$ against $\ln([R]_{to}/[R]_t)$ should be a straight line with a slope of k_1/k_2 and zero intercept.

Experiments were carried out in an evacuable, Teflon-coated 5870 L chamber which is equipped with in situ multiple-reflection optics interfaced to a Nicolet 7199 Fourier transform infrared (FT-IR) spectrometer. Irradiation was provided by a 24 kW xenon arc lamp, with the light being passed through a Pyrex filter to remove wavelengths < 300 nm. Hydroxyl radicals were generated by photolysis of methyl nitrite in air,[10] with NO normally being added to the reactant mixture to suppress the formation of O_3 and hence of NO_3 radicals.[10]

The P-compound was introduced into a small Pyrex bulb (fitted with stopcocks) either as a liquid, with the use of a microliter syringe, or as weighed amount of solid. Due to the known moisture sensitivity of the selected P-compounds, the sample transfers were conducted under an atmosphere of nitrogen. The bulb containing the sample was attached to a chamber inlet and the sample was introduced into the chamber as vapor by heating and flushing with heated N_2 gas. Partial pressures of CH_3ONO, NO, and the reference compound were measured into calibrated 2 L Pyrex bulbs with a 100-Torr MKS Baratron sensor and were introduced by flushing with N_2 into the chamber. All rate constant determinations were conducted in dry diluent air (synthetic mixture of 20% O_2 and 80% N_2, <1% RH) at 298 ± 2 K and 740 Torr total pressure.

Prior to irradiation, the dark decays of the P-compound and the reference compound were monitored for periods of up to 40 min. Depending on the rate of reaction, the irradiations were conducted for total periods ranging from 10 to 40 min. Infrared spectra were recorded every 5 or 10 min prior to and during the irradiation, but as often as every 2 min for the most reactive system. The spectra were taken with 64 scans (corresponding to a 2.0-min averaging time) per spectrum, a full-width-at-half-maximum resolution of 0.7 cm^{-1}, and a path length of 62.9 m.

A limited number of relative rate experiments were also carried out using the rapid reaction of hydrazine with ozone as a nonphotolytic source of OH radicals.[11,12] In this technique, excess O_3 was present in the air mixture of the P-compound and reference compound to which aliquots of N_2H_4 were added to the mixture. Total consumption of the N_2H_4 occurred within 3−5 min after injection and mixing, with the $O_3 + N_2H_4$ reaction producing " short-duration bursts" of OH radicals.[11,12] These experiments are noted in the appropriate sections below.

Product Studies. Experiments were carried out in the 5870 L chamber to investigate the products of the reactions of dimethyl phosphonate and trimethyl phosphite with OH radicals, with analysis by FT-IR absorption spectroscopy and with the photolysis of $CH_3ONO-NO$ and $(CH_3)_2CHONO-NO$[13] mixtures in air as sources of OH radicals. The product study for trimethyl phosphite was extended to include its dark reactions with O_3 and NO_2.

For the reactions of dimethyl phosphonate and trimethyl phosphite with OH radicals, photolyses of P-compound−CH_3ONO−NO mixtures in purified air (~5% RH) were also carried out in a 7500 L Teflon chamber interfaced to a PE SCIEX API III MS/MS direct air sampling atmospheric pressure ionization mass spectrometer (API-MS), with irradiation provided by two parallel banks of blacklamps. The chamber contents were sampled through a 25-mm diameter × 75-cm length Pyrex tube at ~20 L min^{-1} directly into the API-MS source. The positive ion mode was used in the API-MS and API-MS/MS analyses,[14] with protonated water hydrates $[H_3O(H_2O)_n]^+$ generated by the corona discharge in the chamber diluent gas being responsible for the protonation of the analytes. The reactant and product ions that are mass-analyzed are expected to be mainly protonated molecules $([M + H]^+)$ and protonated homo- and hetero-dimers, with the hydrated forms of these species also being observed.[14]

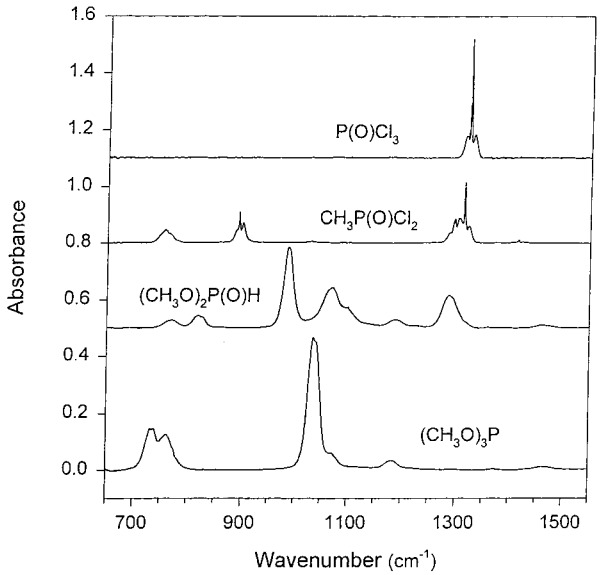

Figure 1. Vapor-phase infrared spectra of phosphorus oxychloride, methylphosphonic dichloride, dimethyl phosphonate, and trimethyl phosphite. All spectra are normalized to concentration = 4.9×10^{13} molecule cm^{-3}; path length = 62.9 m.

Chemicals. The samples of phosphorus oxychloride [$P(O)Cl_3$] (99.999%), methylphosphonic dichloride [$CH_3P(O)Cl_2$] (98%), dimethyl phosphonate [$(CH_3O)_2P(O)H$] (the chemical catalog name is dimethyl phosphite) (98%), and trimethyl phosphite [$(CH_3O)_3P$] (99.999+%) were from Aldrich. The sources and purities of the other chemicals, including the reference compounds used, were nitric oxide (≥99.0%), nitrogen dioxide (≥99.5%), and dimethyl ether (≥99.8%), Matheson Gas Products; tetramethylsilane (99.9+%) and hydrazine (98%), Aldrich; and cyclohexene (99%), Chemical Samples Company.

Methyl nitrite was prepared as described by Taylor et al.[15] and stored under vacuum at 77 K. O_3 in O_2 diluent was prepared using a Welsbach T-408 ozone generator with calibrated settings of voltage and flow of O_2. Dry synthetic air was a mixture of 20% O_2 (Puritan-Bennett Corp., 99.994%) and head gas from liquid N_2 (BOC Gases). Corrections for the presence of N_2O_4 were made to the measured NO_2 partial pressures (typically <4.4 Torr in a 5-L bulb).[16]

Results

Kinetic Studies. *Phosphorus Oxychloride, $P(O)Cl_3$.* Two experiments were carried out using tetramethylsilane as the reference compound, with initial concentrations (in units of 10^{14} molecule cm^{-3}) of $P(O)Cl_3$, 0.59−1.0; $Si(CH_3)_4$, 0.49; and CH_3ONO, 4.9. NO was not added to the reactant mixture in order to maximize the OH radical concentrations during the irradiations. The Q-branches of $P(O)Cl_3$ and $Si(CH_3)_4$ at 1323 and 869 cm^{-1}, respectively, were employed for analysis. The distinct band of $P(O)Cl_3$ at 1323 cm^{-1} is shown in Figure 1, where the strongest IR spectral features of the four P-compounds studied are presented.

In each of the two experiments no detectable change in the initial concentration of $P(O)Cl_3$ was observed during a 40-min period prior to irradiation, during the 34 or 43 min of irradiation, or during the ensuing 40 min after photolysis. The reference compound $Si(CH_3)_4$ showed an ~25% decrease from its initial

TABLE 1: Rate Constant Ratios k_1/k_2 and Rate Constants k_1 for the Reactions of the OH Radical with Selected P-Containing Compounds at 298 ± 2 K

P-compound	reference compound	k_1/k_2[a]	$10^{12} \times k_1$[b] (cm^3 $molecule^{-1}$ s^{-1})	estimated lifetime[c]
phosphorus oxychloride $P(O)Cl_3$	$Si(CH_3)_4$	<0.035[d]	< 0.04[d,e]	>290 days
methylphosphonic dichloride $CH_3P(O)Cl_2$	$Si(CH_3)_4$	0.075 ± 0.023[f]	0.064 ± 0.021[e]	180 days
dimethyl phosphonate $(CH_3O)_2P(O)H$	$(CH_3)_2O$	1.79 ± 0.06	5.08 ± 0.53[g]	2.3 days
trimethyl phosphite $(CH_3O)_3P$	cyclohexene	10.5 ± 0.8	710 ± 90[h]	0.016 day

[a] Indicated errors are two least-squares standard deviations, unless noted otherwise. [b] Total errors given take into account the uncertainties of the rate constants k_2. [c] Calculated on the basis of a 24-h average OH radical concentration of 1×10^6 molecule cm^{-3}. [17,18] [d] Upper limit estimate (see text). [e] Placed on an absolute basis using $k_2[OH + Si(CH_3)_4] = (8.5 \pm 0.9) \times 10^{-13}$ cm^3 $molecule^{-1}$ s^{-1} at 298 K.[12] [f] See text. Two least-squares standard deviations are ±0.013. [g] Placed on an absolute basis using $k_2[OH + (CH_3)_2O] = 2.84 \times 10^{-12}$ cm^3 $molecule^{-1}$ s^{-1} at 298 K,[19] with an estimated overall uncertainty of ±10%.[20] [h] Placed on an absolute basis using $k_2[OH + cyclohexene] = 6.77 \times 10^{-11}$ cm^3 $molecule^{-1}$ s^{-1} at 298 K,[21,22] with an estimated overall uncertainty of ±10%.[20]

concentration after 22−23 min of irradiation, with a total loss of ∼28% for the entire irradiation periods. Although no reaction of $P(O)Cl_3$ was observed, an upper limit to the OH radical rate constant for $P(O)Cl_3$ can be estimated from the minimum detectable change in its concentration. The interactive, subtractive comparison of the initial band intensity of $P(O)Cl_3$ at 1323 cm^{-1} with those of the subsequent spectra indicated that a concentration change of 0.5% was detectable. For an estimate of an upper limit to the rate constant k_1, we assign an upper limit of 1% consumption of $P(O)Cl_3$ (twice the minimum detectable change) combined with a 25% consumption of the reference $Si(CH_3)_4$. The upper limits to the rate constant ratio k_1/k_2 and the rate constant k_1 are given in Table 1.

In an attempt to obtain higher concentrations of OH radicals, an experiment which employed the $O_3 + N_2H_4$ reaction as the source of OH radicals was carried out, with initial concentrations (10^{14} molecule cm^{-3}) of $P(O)Cl_3$, 0.59; $Si(CH_3)_4$, 0.49; O_3, 4.8; and N_2H_4, 1.2. No measurable losses of either $P(O)Cl_3$ or $Si(CH_3)_4$ were observed in their initial mixture with O_3 during a 40-min period. A 25% loss of the initial $P(O)Cl_3$ was observed after N_2H_4 injection to the $P(O)Cl_3-Si(CH_3)_4-O_3$ mixture, together with an observed 9% loss of $Si(CH_3)_4$. As expected in the presence of excess O_3, N_2H_4 was rapidly and totally consumed. However, the spectra showed no absorption bands of H_2O or H_2O_2, which are products of the $O_3 + N_2H_4$ reaction.[11] The observed loss of $P(O)Cl_3$ is attributed to its reaction/condensation with H_2O, H_2O_2, and most likely N_2H_4, instead of reaction with OH radicals generated from the $O_3 + N_2H_4$ reaction. The appearance of broad, featureless bands in the IR spectrum of the reaction mixture was further indication that condensation products were formed. Hence, this OH radical generation technique is not suited for the OH radical rate constant measurement for $P(O)Cl_3$.

Methylphosphonic Dichloride, $CH_3P(O)Cl_2$. Four experiments were carried out using $Si(CH_3)_4$ as the reference compound, with initial concentrations (10^{14} molecule cm^3) of $CH_3P(O)Cl_2$, 1.2−1.7; $Si(CH_3)_4$, 0.73; and CH_3ONO, 4.9. As in the experiments with $P(O)Cl_3$, NO was not added to the initial reactant mixtures. The absorption bands of $CH_3P(O)Cl_2$ and $Si(CH_3)_4$ with distinct Q-branches at 893 and 869 cm^{-1}, respectively, were employed for analysis (see Figure 1).

The dark decays of $CH_3P(O)Cl_2$ and $Si(CH_3)_4$ were monitored for 40 min before and after irradiation. The concentration of $CH_3P(O)Cl_2$ in the mixture of reactants decayed slowly prior to the irradiation, with rates ranging from being immeasurable during a 40-min period to an observed decay rate of 6.5×10^{-4} min^{-1}. The $CH_3P(O)Cl_2$ decay rate in the dark after irradiation was in the range $(5.0-8.0) \times 10^{-4}$ min^{-1}. $Si(CH_3)_4$ exhibited no measurable decay before or after the photolysis period.

The 40-min photolysis of $CH_3P(O)Cl_2-Si(CH_3)_4-CH_3ONO-$air mixtures showed $CH_3P(O)Cl_2$ losses of only 3−4.5% of its initial concentrations. The consumption of $Si(CH_3)_4$ for the same period amounted to ∼28% of the initial concentration, but for each experiment ∼85% of the total amount of $Si(CH_3)_4$ consumed occurred during the first 25 min of irradiation. Only the measurements within this 25-min photolysis period are included in the data analysis in order to minimize any influence of photolysis products on the consumption of $CH_3P(O)Cl_2$. For each experiment, the measured $CH_3P(O)Cl_2$ concentrations during the photolysis were corrected for losses using the decay rate determined prior to irradiation. The data from four separate experiments, corrected for $CH_3P(O)Cl_2$ self-decay, are plotted according to eq I in Figure 2. The rate constant ratio k_1/k_2 obtained from a least-squares analysis of these data is given in Table 1 along with the rate constant k_1. Because the observed small changes in the $CH_3P(O)Cl_2$ concentration are near the measurement limit (differences in $CH_3P(O)Cl_2$ concentrations <0.25−0.50% could not be detected using FT-IR analysis), an overall uncertainty of ±30% is assigned to the rate constant ratio k_1/k_2 (Table 1).

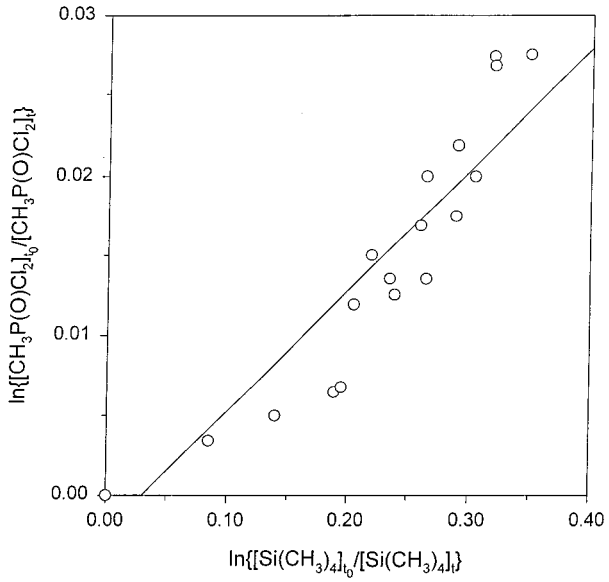

Figure 2. Plot of eq I for the reactions of $CH_3P(O)Cl_2$ and $Si(CH_3)_4$ with the OH radical. The data plotted are from four separate experiments.

As in the case of $P(O)Cl_3$, the rapid dark reaction of hydrazine with ozone, which yields higher "short bursts" of OH radicals[11,12] and hence potentially higher incremental reactant consumptions, was also used. It was likewise unsuccessful, presumably due to the condensation of $CH_3P(O)Cl_2$ with hydrazine (also suggested by the occurrence of very broad, structureless IR absorption bands), since $CH_3P(O)Cl_2$ has been

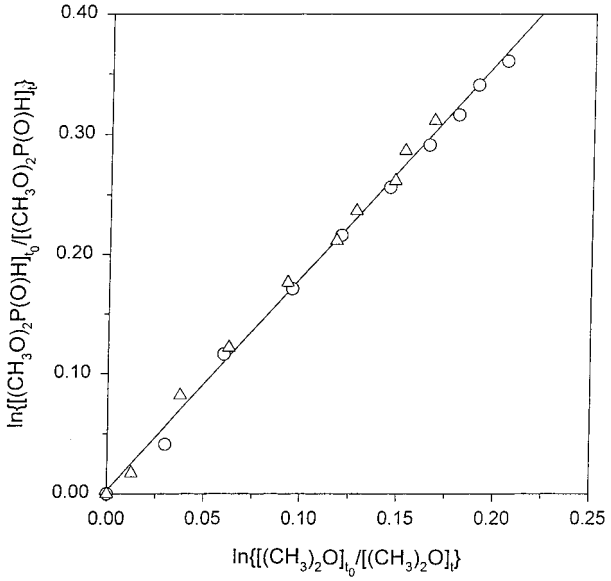

Figure 3. Plot of eq I for the reactions of $(CH_3O)_2P(O)H$ and $(CH_3)_2O$ with the OH radical. The data plotted are from two separate experiments.

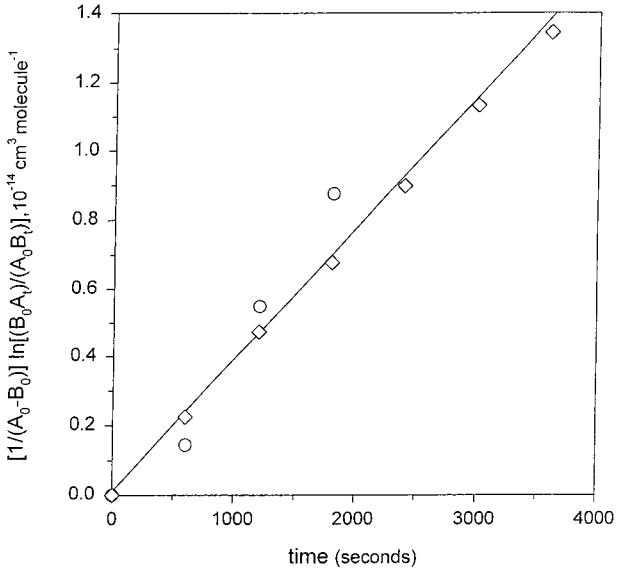

Figure 4. Plot of eq II for the reaction of NO_2 with $(CH_3O)_3P$, where *A* and *B* represent their respective concentrations. Data for two separate experiments are plotted with initial concentrations (in units of 10^{13} molecule cm^{-3}) of circles, $A_0 = 6.11$ and $B_0 = 5.88$; diamonds, $A_0 = 11.36$ and $B_0 = 5.54$.

reported to undergo condensation reactions with aminobenzenes[23] and alcohols.[24]

Dimethyl Phosphonate, $(CH_3O)_2P(O)H$. Two experiments were carried out using dimethyl ether as the reference compound. The initial reactant concentrations employed (in units of 10^{14} molecule cm^{-3}) were $(CH_3O)_2P(O)H$, 1.1; $(CH_3)_2O$, 2.5; CH_3ONO, 4.9; and NO, 1.5−1.8. The dark decays of $(CH_3O)_2P(O)H$ and $(CH_3)_2O$ were monitored for 40 min before and after irradiation. The absorption bands of $(CH_3O)_2P(O)H$ and $(CH_3)_2O$ at 987 and 1178 cm^{-1}, respectively, were employed for analysis (Figure 1). For an accurate analysis of these bands, it was necessary to subtract the absorption bands of unreacted CH_3ONO and of other photooxidation products, i.e., HCHO, HNO_3, and CH_3ONO_2 formed from CH_3ONO and NO, and CH_3OCHO formed from $(CH_3)_2O$.[21]

The concentration of $(CH_3O)_2P(O)H$ in the mixture of reactants decayed slowly prior to and after irradiation, and these dark decay rates were in the range $(4.9-6.6) \times 10^{-4}$ min^{-1}. The average of the $(CH_3O)_2P(O)H$ decay rates before and after irradiation was 5.5×10^{-4} min^{-1} in the first experiment and 5.0×10^{-4} min^{-1} in the second experiment carried out. $(CH_3)_2O$ exhibited no measurable dark decay before or after photolysis.

The 40-min photolyses of $(CH_3O)_2P(O)H-(CH_3)_2O-CH_3ONO-NO-$air mixtures showed $(CH_3O)_2P(O)H$ losses of ∼26% of its initial concentration, while the consumption of $(CH_3)_2O$ for the same period amounted to ∼15% of its initial concentration. For each of the two experiments, the measured $(CH_3O)_2P(O)H$ concentrations during the photolysis were corrected for losses due to self-decay using the average decay rates noted above. The combined data from the two irradiation experiments are plotted according to eq I in Figure 3. The effect of the small corrections due to the $(CH_3O)_2P(O)H$ dark decays on the value of k_1/k_2 was negligible. The rate constant ratio k_1/k_2 and the rate constant k_1 obtained are given in Table 1.

Trimethyl Phosphite, $(CH_3O)_3P$. Two experiments were carried out to measure the OH radical reaction rate constant, using cyclohexene as the reference compound. The initial reactant concentrations (10^{14} molecule cm^{-3}) employed were $(CH_3O)_3P$, 0.62; cyclohexene, 4.9; CH_3ONO, 2.5; and NO, 2.5. Experiments were also carried out to measure the photolysis rate of $(CH_3O)_3P$ in air at the light intensity used for the OH radical reaction experiments and to determine the rate constant for an observed reaction between $(CH_3O)_3P$ and NO_2. All reactions were conducted at 298 ± 2 K and 740 Torr total pressure of diluent air, except the $NO_2 + (CH_3O)_3P$ experiments which employed mixtures of the reactants in N_2. IR spectra were recorded every 5 min, with a 2.0-min averaging time per spectrum, during the $(CH_3O)_3P$ photolysis, dark decay, and reaction with NO_2, while spectra were taken at intervals as short as every 2.1 min during the OH radical rate constant measurements. The absorption bands of $(CH_3O)_3P$ at 735 and 1037 cm^{-1} (Figure 1), of cyclohexene at 1140 cm^{-1}, and of NO_2 at 1617 cm^{-1} were employed for analysis.

The decay rates of $(CH_3O)_3P$ as measured in dry air for periods of up to 40 min at the beginning of the experiments were negligible, being $\leq 2 \times 10^{-4}$ min^{-1}. However, $(CH_3O)_3P$ was observed to photolyze appreciably in air and to decay significantly in its air mixture with CH_3ONO and NO in the dark. A photolysis rate for $(CH_3O)_3P$ of 2.2×10^{-3} min^{-1} was measured over a 56-min irradiation period (initial concentration of $(CH_3O)_3P$ of 4.9×10^{13} molecule cm^{-3}) for the light intensity employed in all experiments involving irradiation. The decay of $(CH_3O)_3P$ in its mixture with CH_3ONO and NO in air was found to be due to its reaction with the NO_2 formed from the thermal oxidation of NO in air. It was verified in separate experiments that $(CH_3O)_3P$ did not react with CH_3ONO, NO (conducted in N_2 diluent), or gaseous HNO_3.

The rate constant k_{NO_2} for the $NO_2 + (CH_3O)_3P$ reaction was determined from experiments where the time dependence of the concentrations of both reactants was measured. The data obtained were plotted according to the integrated second-order rate equation

$$[1/(A_0 - B_0)] \ln[(B_0A_t)/(A_0B_t)] = k_{NO_2}t \qquad \text{(II)}$$

where A_0 and B_0 are the concentrations of NO_2 and $(CH_3O)_3P$, respectively, at time t_0, and A_t and B_t are the corresponding concentrations at time *t*. Data from two experiments are combined in the plot of eq II shown in Figure 4. The experiment represented by the open circles involved $(CH_3O)_3P$ and NO in N_2 diluent with subsequent addition of NO_2. The rate constant

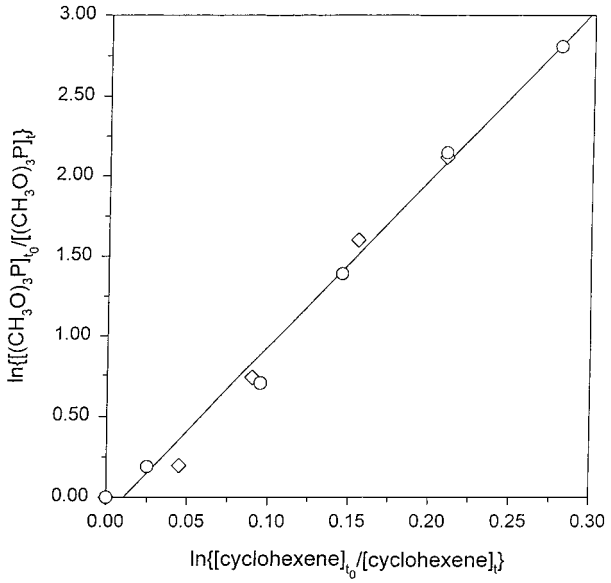

Figure 5. Plot of eq I for the reactions of $(CH_3O)_3P$ and cyclohexene with the OH radical. The data plotted are from two separate experiments.

for reaction of $(CH_3O)_3P$ with NO_2 obtained from least-squares analysis of the data shown in Figure 4 is $k_{NO_2} = (3.8 \pm 0.4) \times 10^{-18}$ cm^3 molecule^{-1} s^{-1}, with the quoted error being two least-squares standard deviations.

The measured $(CH_3O)_3P$ photolysis rate and NO_2 reaction rate constant were then used to correct the measured $(CH_3O)_3P$ concentrations during the $CH_3ONO-NO-$air photolyses to determine the OH radical rate constant. Cyclohexene, the reference compound, showed no detectable losses in the reaction mixture prior to irradiation. Two experiments were carried out, one employed continuous irradiation with spectra being recorded every 2.1 min over a total period of ~10 min; the second employed intermittent photolyses of 2.0 min per irradiation, with spectra being recorded during the intervening dark periods for a total experiment time of ~20 min. The spectral data collected during the experiment with continuous irradiation were in the form of interferograms, which were then converted to spectra after the irradiation.

Corrections of the observed $(CH_3O)_3P$ consumption at time t due to reaction with NO_2 were calculated using the rate constant k_{NO_2} determined here, the time $(t_i - t)$ between two spectral records, the $(CH_3O)_3P$ concentration measured at t_i, and the NO_2 concentration determined at the later time t. Since the NO_2 concentration increased during the irradiation, therefore during the period $(t_i - t)$ the corrections applied to take into account reaction with NO_2 were upper-limit estimates. The upper-limit contribution of photolysis to the $(CH_3O)_3P$ loss during the period $(t_i - t)$ was calculated from the $(CH_3O)_3P$ concentration at t_i and the measured photolysis rate (see above). No corrections were applied to the measured cyclohexene concentrations.

The combined data from the two irradiation experiments, with corrections to the $(CH_3O)_3P$ concentrations, are plotted according to eq I in Figure 5. The rate constant ratio k_1/k_2 and the rate constant k_1 obtained are given in Table 1. Corrections for photolysis and reaction with NO_2 were small, changing the slope of the plot by ~5% for the continuous irradiation experiment and by ~13% for the intermittent irradiation experiment.

Due to the observed photolysis of $(CH_3O)_3P$ and its reaction with NO_2 produced in the $CH_3ONO-NO$ mixture, the use of the relative rate technique employing the $N_2H_4 + O_3$ reaction as source of OH radicals[11,12] was considered. However, $(CH_3O)_3P$ was observed to react rapidly with O_3; in an experiment where 7.4×10^{13} molecule cm^{-3} of O_3 was added to an air mixture containing 6.5×10^{13} molecule cm^{-3} of $(CH_3O)_3P$, >97% of the $(CH_3O)_3P$ had reacted after a 2-min mixing time, corresponding to a lower limit to the O_3 reaction rate constant of $\geq 4 \times 10^{-16}$ molecule^{-1} s^{-1}. An attempt was also made to use the photolysis of H_2O_2 as the OH radical source, but condensation of $(CH_3O)_3P$ with either or both of H_2O_2 and H_2O (the reagent being a 50:50 mixture) occurred prior to and during irradiation, as indicated by the appearance of broad absorption bands in the IR spectra of the reaction mixture.

Product Studies. *Reactions of Trimethyl Phosphite.* The photolysis of $(CH_3O)_3P$ and its reactions with NO_2 and O_3 were examined for any products formed and their yields. Trimethyl phosphate $[(CH_3O)_3PO]$ was the only product detected by FT-IR analysis during photolysis, with a yield of 88 ± 9%. FT-IR analysis showed that unit yields of $(CH_3O)_3PO$ were formed from $(CH_3O)_3P$ during the $(CH_3O)_3P + NO_2$ and $(CH_3O)_3P + O_3$ reactions described above, with a 1:1 stoichiometry of reactants in both cases.

Irradiation of $(CH_3O)_3P-CH_3ONO-NO-$air and $(CH_3O)_3P-(CH_3)_2CHONO-NO-$air mixtures were carried out to identify the products of the $(CH_3O)_3P + OH$ reaction. Initial concentrations (10^{14} molecule cm^{-3}) similar to those for the kinetic experiments (less the reference compounds) were employed: $(CH_3O)_3P$, 0.63−0.74; NO, 2.5; and CH_3ONO, 2.5, or $(CH_3)_2CHONO$, 2.0. During a 65-min dark period, the initial $(CH_3O)_3P-CH_3ONO-NO-$air mixture was observed to form 1.7×10^{13} molecule cm^{-3} of $(CH_3O)_3PO$, with a corresponding equal loss of $(CH_3O)_3P$, due to dark reaction with NO_2 formed from thermal oxidation of NO. Upon photolysis, the consumption of the initial 4.6×10^{13} molecule cm^{-3} of $(CH_3O)_3P$ prior to irradiation was 51% after 2 min and 89% after 5 min. Spectra of products attributed to $(CH_3O)_3P$ were obtained after subtraction of absorptions by NO_2, HONO, HNO_3, HCOOH, CH_3ONO_2, and HCHO (for the latter two, the corresponding bands of $(CH_3)_2CHONO_2$ and $(CH_3)_2CO$ were subtracted in the experiment where $(CH_3)_2CHONO$ photolysis was employed). Figure 6A shows the product spectrum after 2 min of irradiation, where $(CH_3O)_3PO$ is identified as the major product and its concentration corrected for the amount formed prior to photolysis. HCHO was also observed as a product and was measured quantitatively from the spectra recorded, using its distinct 1745 cm^{-1} absorption peak (not illustrated), from the photolysis of a $(CH_3O)_3P-(CH_3)_2CHONO-NO-$air mixture. The latter photolysis experiment consisted of five 1-min irradiations, with spectra being recorded during the intervening dark periods. The yields of $(CH_3O)_3PO$ were also monitored in this experiment and combined with those from the irradiation which employed CH_3ONO photolysis as source of OH radicals. It was verified from separate irradiations of $(CH_3)_2CHONO-NO-$air mixtures that the amounts of HCHO formed from $(CH_3)_2CHONO$ at comparable time periods (≤5 min) were negligible.

Figure 7 shows a plot of the amounts of $(CH_3O)_3PO$ and HCHO formed against the amounts of $(CH_3O)_3P$ consumed by reaction with OH radicals. The observed $(CH_3O)_3PO$ and HCHO concentrations were corrected for their reaction with OH radicals[25] using OH radical reaction rate constants (cm^3 molecule^{-1} s^{-1}) of HCHO, 9.3×10^{-12};[19,21] $(CH_3O)_3PO$, 7.4×10^{-12}; [6] and $(CH_3O)_3P$, 7.1×10^{-10} (this work). The corrections to the HCHO and $(CH_3O)_3PO$ concentrations due to secondary reactions with OH radicals were ≤2% and ≤4%, respectively.

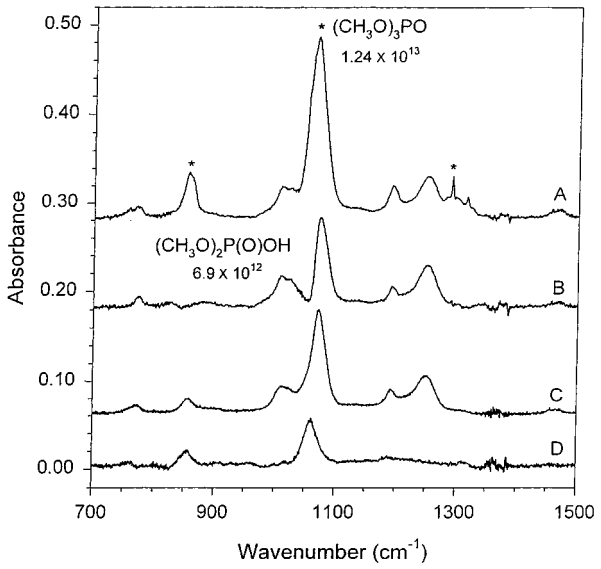

Figure 6. (A) Product spectrum from a $(CH_3O)_3P-CH_3ONO-NO-$air photolysis. (B) Residual spectrum from (A) after subtraction of absorptions by $(CH_3O)_3PO$, showing mainly absorptions by $(CH_3O)_2P(O)OH$. (C) Spectrum of a commercial sample of $(CH_3O)_2P(O)OH$ with absorptions by $(CH_3O)_3PO$ and CH_3OH impurities subtracted. (D) Residual spectrum from (C) after a proportionate subtraction of (B), showing bands from another impurity in the commercial sample of $(CH_3O)_2P(O)OH$. Numbers indicated are concentrations in molecule cm^{-3}. See text for details.

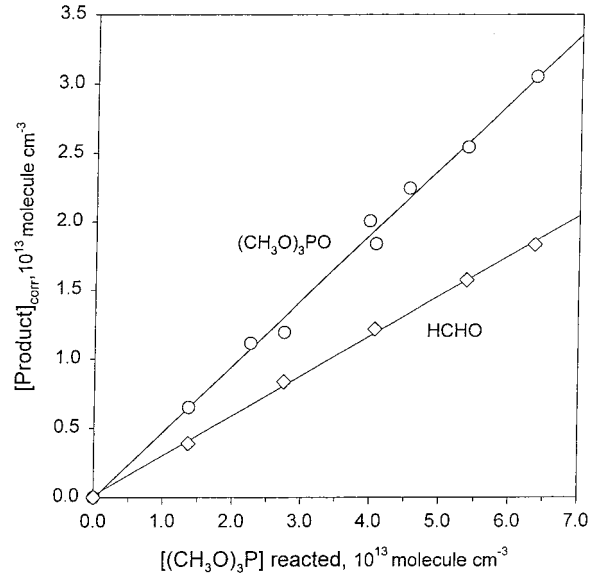

Figure 7. Yield plots of trimethyl phosphate and formaldehyde from the trimethylphosphite + OH reaction. $(CH_3O)_3PO$ and HCHO concentrations were corrected for secondary reactions with the OH radical; corrections for $(CH_3O)_3P$ reacted and $(CH_3O)_3PO$ formed from $(CH_3O)_3P$ "photolysis" and $(CH_3O)_3P + NO_2$ reaction were applied (see text).

Corrections to the measured $(CH_3O)_3PO$ concentrations to take into account formation from $(CH_3O)_3P$ photolysis and the $(CH_3O)_3P + NO_2$ reaction were included and the equivalent corrections from these two processes were also applied to the amounts of $(CH_3O)_3P$ consumed on the basis of a 1:1 yield of $(CH_3O)_3PO$ from $(CH_3O)_3P$. The combined corrections due to $(CH_3O)_3P$ photolysis and $(CH_3O)_3P + NO_2$ reaction amounted to 0.4−7% of the $(CH_3O)_3P$ losses and 1−15% of the $(CH_3O)_3PO$ formed, where the few data points with the higher corrections occurred in the experiment with intermittent irradiation due to the additional $(CH_3O)_3P + NO_2$ reaction which occurred during the intervening dark periods. A least-squares analysis of the data shown in Figure 7 leads to formation yields of 0.48 ± 0.05 for $(CH_3O)_3PO$ and 0.29 ± 0.03 for HCHO, where the errors cited are the total of the two least-squares standard errors and those arising from uncertainties in the FT-IR analyses of reactant and products.

Subtraction of the absorptions of $(CH_3O)_3PO$ from Figure 6A revealed the presence of another product, as seen in Figure 6B. The absorption features in Figure 6B are very similar to those of a spectrum of dimethyl phosphate $[(CH_3O)_2P(O)OH]$ shown in Figure 6C, the latter being derived from the spectrum of a commercial sample after subtraction of absorptions by the identifiable impurities [analyzed as 22% by wt $(CH_3O)_3PO$ and 1.2% by wt CH_3OH]. A subtractive comparison of the dimethyl phosphate spectrum from the irradiation experiment (Figure 6B) with that from the commercial sample (Figure 6C) revealed another impurity in the commercial product with its strongest absorption band at 1062 cm^{-1} (Figure 6D). The presence of this unidentified component was also deduced from the time behavior of the commercial sample spectra as observed separately in the chamber because of a difference between the decay rates of dimethyl phosphate (~0.02 min^{-1}) and of the unknown component. No reliable calibration was obtained for dimethyl phosphate from the commercial sample. A consideration of possible chemical mechanisms (cf. below) suggests that the $(CH_3O)_2P(O)OH$ yield from $(CH_3O)_3P$ should be equal to the yield of HCHO. When the latter was assumed as a basis of calibration, the amount of $(CH_3O)_2P(O)OH$ initially in the vapor phase corresponded to only about 9% by wt of the commercial sample introduced into the chamber.

Photolysis of an air mixture containing 1.2×10^{13} molecule cm^{-3} each of $(CH_3O)_3P$, CH_3ONO, and NO was carried out in the 7000-L Teflon chamber with API-MS analyses. The API-MS spectrum of trimethyl phosphite showed a strong protonated parent peak, $[M_T + H]^+ = 125$ u. After addition of CH_3ONO and NO and prior to irradiation, a weak peak was observed at 265 u, corresponding to the protonated hetero-dimer $[M_T + M_{P1} + H]^+$, where $M_{P1} = 140$ is the molecular weight of $(CH_3O)_3PO$ formed from the reaction of trimethyl phosphite with the small amounts of NO_2 formed from NO. Figure 8, top panel, shows the API-MS spectrum of the $(CH_3O)_3P-CH_3ONO-NO-$air mixture after two irradiations of 15-s duration each at 20% of maximum light intensity. A marked increase in the intensity of the 265-u peak was observed during the irradiations. In addition, ion peaks at 141, 235, 251, and 281 u were observed (Figure 8) and API-MS/MS "product ion" spectra of these ion peaks and that at 265 u were obtained. The API-MS/MS "product ion" spectra indicated that the 265- and 281-u ion peaks were $[M_T + M_{P1} + H]^+$ and $[M_{P1} + M_{P1} + H]^+$, respectively, and that the 235- and 251-u ion peaks could be $[M_T + M_{P2} + H]^+$ and $[M_{P1} + M_{P2} + H]^+$, respectively, where M_{P2} is a molecular weight 110 product (although the 235- and 251-u ion peaks could also be fragments of the 265- and 281-u ion peaks).

Dimethyl Phosphonate + OH. Irradiations of $(CH_3O)_2P(O)H-CH_3ONO-NO-$air and $(CH_3O)_2P(O)H-(CH_3)_2CHONO-NO-$air mixtures were carried out, with initial concentrations (10^{14} molecule cm^{-3}): $(CH_3O)_2P(O)H$, 1.1; NO, 2.5; and CH_3ONO, 2.5, or $(CH_3)_2CHONO$, 2.0. Figures 9A−9C are residual spectra which show weak absorption bands of products attributed to dimethyl phosphonate (after subtraction of absorptions from a number of species as noted above for the case of trimethyl phosphite), formed after 4, 34, and 64 min during the irradiation

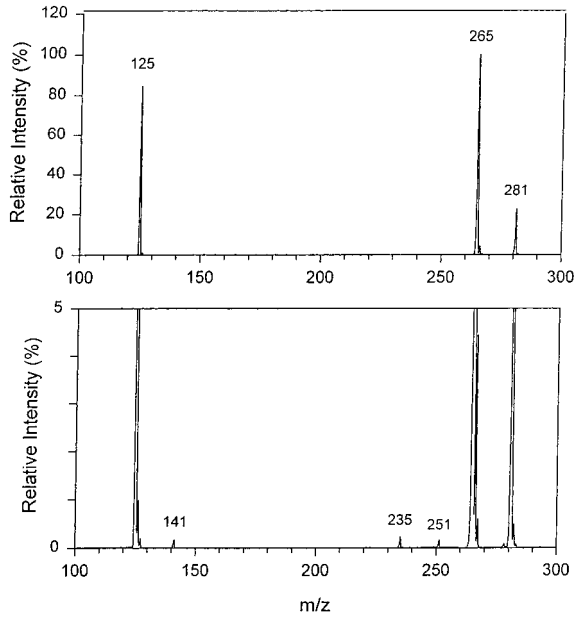

Figure 8. Top: API-MS spectrum of an irradiated $(CH_3O)_3P-CH_3ONO-NO-$air mixture. Bottom: Above spectrum with 20-fold ordinate expansion.

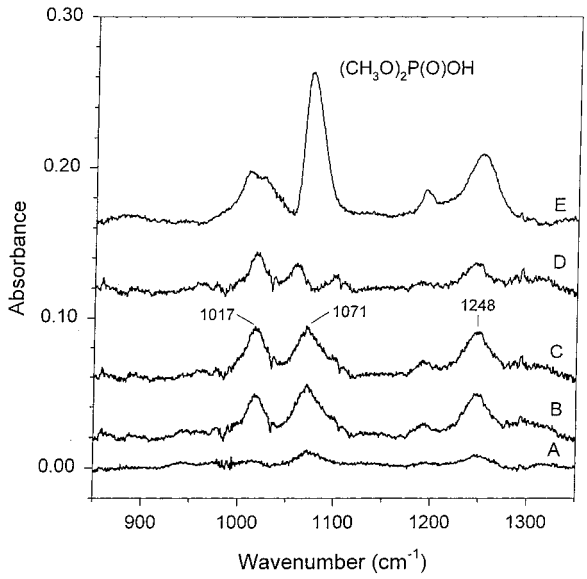

Figure 9. Product spectra from a $(CH_3O)_2P(O)H-CH_3ONO-NO-$air photolysis after (A) 4 min, (B) 34 min, and (C) 64 min of irradiation. The residual spectrum (D) resulted from a proportionate subtraction of the $(CH_3O)_2P(O)OH$ spectrum shown in (E). See text for details.

of a $(CH_3O)_2P(O)H-CH_3ONO-NO-$air mixture and corresponding to 3.5%, 21%, and 28% consumption, respectively, of the initial dimethyl phosphonate. The absorption band at 1248 cm^{-1} is consistent with the presence of a P═O group, while the bands at 1017 and 1071 cm^{-1} are in the range associated with the P−O−C group(s).[26,27] The development of the 1017 cm^{-1} absorption lagged that of the 1071 cm^{-1} band in the early part of the reaction, indicating the formation of at least two products. The product spectra in the early stage of the reaction bear some similarity to the spectrum of dimethyl phosphate. Figure 9D shows the remaining absorption bands after subtraction from Figure 9C of the probable contribution from $(CH_3O)_2P(O)OH$ (Figure 9E; from Figure 6B). Adopting the calibration for $(CH_3O)_2P(O)OH$ obtained for the case of trimethyl phosphite, the probable yield of $(CH_3O)_2P(O)OH$ from dimethyl phosphonate obtained after 4 min of irradiation (3.5% reaction)

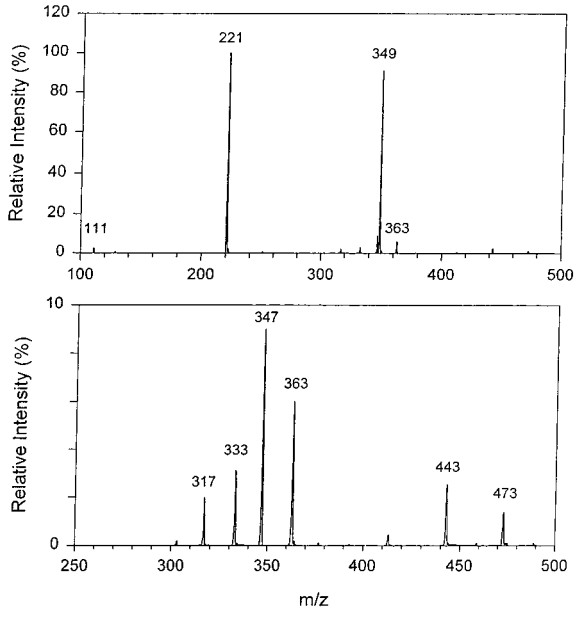

Figure 10. Top: API-MS spectrum of an irradiated $(CH_3O)_2P(O)H-CH_3ONO-NO$ −air mixture. Bottom: Above spectrum scale-expanded after subtracting the spectrum of the initial mixture.

was 15%, which progressively decreased to 7% after 64 min of irradiation (28% reaction).

No well-defined absorption bands in the C═O stretch region were observed that could be attributed to products of dimethyl phosphonate. HCHO was observed during the photolysis of a $(CH_3O)_2P(O)H-(CH_3)_2CHONO-NO$ air mixture, but the amounts formed corresponded to the 2−3% yield from $(CH_3)_2CHONO$ that was observed during the irradiation of air mixtures of $(CH_3)_2CHONO-NO$ alone under the same light intensity and duration of photolysis. Thus, the relatively minor amounts of HCHO observed were attributed mainly or totally to formation from $(CH_3)_2CHONO$.

Figure 10, top panel, shows the API-MS spectrum of an irradiated $(CH_3O)_2P(O)H-CH_3ONO-NO-$air mixture, with initial concentrations of 2.4×10^{13} molecule cm^{-3} of each reactant, after 5 min of photolysis at 20% of maximum light intensity. The ion peaks at 111, 221, and 349 u, which were also the dominant peaks in the API-MS spectrum of the mixture before irradiation, are assigned to $[M_D + H]^+$, $[M_D + M_D + H]^+$, and $[M_D + M_D + M_D + H_3O]^+$, where $M_D = 110$ is the molecular weight of dimethyl phosphonate. The peaks which appeared at 317, 333, 347, 363, 443, and 473 u after irradiation, more clearly seen in Figure 10, bottom panel, after subtraction of the initial peaks and scale expansion, are attributed to the formation of the protonated hetero-dimers, -trimers, and -tetramers, and are assigned to: 317 u, $[M_D + M_D + M_{P1} + H]^+$; 333 u, $[M_D + M_{P1} + M_{P2} + H]^+$; 347 u, $[M_D + M_D + M_{P2} + H]^+$; 363 u, $[M_D + M_{P2} + M_{P2} + H]^+$; 443 u, $[M_D + M_D + M_{P1} + M_{P2} + H]^+$; and 473 u, $[M_D + M_D + M_{P2} + M_{P2} + H]^+$, where $M_{P1} = 96$ and $M_{P2} = 126$. M_{P2} is consistent with the formation of dimethyl phosphate, a product suggested but not conclusively identified in the experiments with FT-IR analysis. The possibility that the product P_1 with molecular weight 96 is methyl phosphonate is discussed below.

Discussion

Using the room-temperature rate constants k_1 given in Table 1, the lifetimes τ of the P-containing compounds studied in the troposphere can be estimated from the expression $\tau = (k_1[OH])^{-1}$, where [OH] is the hydroxyl radical concentration. Using a 24-h

average OH radical concentration of 1×10^6 molecule cm^{-3},[17,18] the calculated tropospheric lifetimes of these P-compounds with respect to reaction with the OH radical are given in Table 1.

It is likely that the atmospheric lifetimes of these selected P-compounds will be shorter (maybe appreciably shorter) than the estimated gas-phase lifetimes due to reaction with OH radicals alone. The pure samples have varying affinities for reaction/condensation with water, with, for example, the solid $CH_3P(O)Cl_2$ being visibly deliquescent. As observed during the experiments where the $O_3 + N_2H_4$ reaction and H_2O_2 photolysis were attempted as alternative sources of OH radicals, these P-compounds appear to undergo possible condensation with compounds bearing hydroxyl and amino groups. Since atmospheric particulates are bound to possess entities with such functional groups, incorporation into aerosols (and subsequent washout) along with wet deposition from the gas phase are expected to be significant, additional removal pathways for these P-compounds in the atmosphere. In the case of $(CH_3O)_3P$, given its observed rapid reaction with O_3 [only a lower limit to the rate constant for the $O_3 + (CH_3O)_3P$ reaction was measured in this study] and reaction with NO_2, its atmospheric gas-phase lifetime will be shorter than that calculated for reaction with the OH radical alone. For assumed ambient O_3 and NO_2 concentrations of 7×10^{11} molecule cm^{-3} (30 ppb) and 2.4×10^{10} molecule cm^{-3} (1 ppb), respectively, the lifetimes of $(CH_3O)_3P$ due to reactions with O_3 and NO_2 are calculated to be <1 h and 125 days, respectively, showing that under typical tropospheric conditions the NO_2 reaction will be of no importance, while the O_3 reaction could be important, especially at night.

The reactions of triaryl and trialkyl phosphites, including $(CH_3O)_3P$, with O_2, O_3, and NO_2 (or N_2O_4) in the liquid phase and/or in solution have been shown to give near quantitative yields of trialkyl phosphates.[28,29] In dilute solutions the phosphite−ozone stoichiometry is 1:1,[29] consistent with the stoichiometry observed here for the gas-phase reactions of $(CH_3O)_3P$ with O_3 and NO_2 to form $(CH_3O)_3PO$. The present data do not give any indication of a mechanism other than effectively a direct transfer of O atom to the trimethyl phosphite P atom to form $(CH_3O)_3PO$ and O_2 and NO, respectively, for the reactions with O_3 and NO_2. The observed acceleration of $(CH_3O)_3P$ air oxidation ($<2 \times 10^{-4}$ min^{-1} to 2×10^{-3} min^{-1}) upon UV irradiation in the present experiments has also been observed for liquid samples of trialkyl phosphites,[28] which was attributed to formation of radicals ($RO_2^{\bullet}$ and $RO^{\bullet}$) from organic impurities. Since trialkyl phosphites do not absorb significantly in the actinic region,[30] the observed enhanced air oxidation of $(CH_3O)_3P$ is consistent with the known formation of radicals from trace impurities in chambers during irradiation experiments.[31]

For the gas-phase reaction of trimethyl phosphite with the OH radical, formation of an adduct is the likely initial step toward formation of the observed major products, as shown in Scheme 1. The experiments carried out with FT-IR and API-MS analyses showed $(CH_3O)_3PO$ to be the major product, but the FT-IR detection and indication of appreciable amounts of $(CH_3O)_2P(O)OH$ formed (as equated to the observed HCHO yield) is not supported by API-MS analysis, which did not detect ion peaks associated with dimethyl phosphate. However, the API-MS spectra indicated the possible formation of a species of molecular weight 110, most likely a minor product (which is not detected in the runs with FT-IR analysis), and is believed to be dimethyl phosphonate. Displacement of a methoxy group from trimethyl phosphite by OH radical attack on the P atom

SCHEME 1

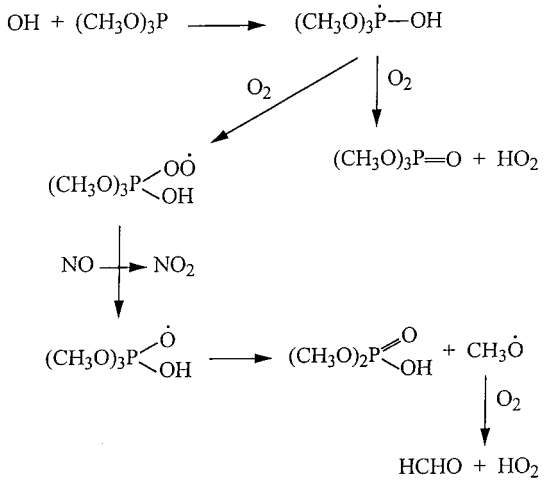

SCHEME 2

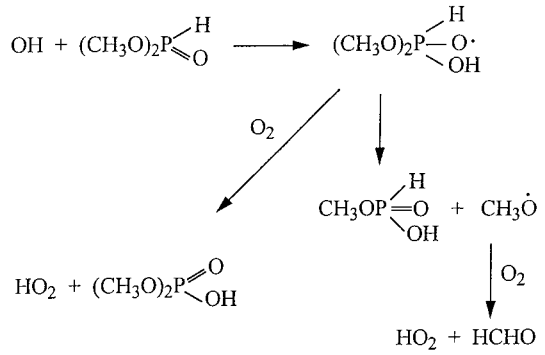

could result in the formation of dimethyl phosphite initially in its tervalent form, followed by rapid conversion to the energetically favored phosphonate form, dimethyl phosphonate:

$$(CH_3O)_3P + OH \rightarrow (CH_3O)_2P{-}OH + CH_3O^{\bullet}$$
$$(CH_3O)_2P{-}OH \rightarrow (CH_3O)_2P(=O)H$$

The possibility that dimethyl phosphate could also form from trimethyl phosphate by a direct displacement reaction was judged to be unimportant, since it was not observed during a previous product study of the $(CH_3O)_3PO + OH$ reaction.[6]

The reaction of dimethyl phosphonate with the OH radical could proceed via initial addition of the OH radical to the P atom, followed by reaction with O_2 to form dimethyl phosphate and/or displacement of a methoxy group leading to the formation of methyl phosphonate, as shown in Scheme 2. As noted above, the observed yield of HCHO which would form from the methoxy radical was not significant, suggesting that methyl phosphonate was, at most, a minor product.

The FT-IR quantification of the trimethyl phosphite + OH reaction products accounts for 77 ± 6% of the trimethyl phosphite reacted. The FT-IR analysis for the dimethyl phosphonate + OH reaction is less definitive both qualitatively and quantitatively.

Note Added in Proof. After this work was completed, we became aware of the study of Kleindienst and Smith (Chemical Degradation in the Atmosphere, Final Report on the Atmospheric Chemistry of Three Important Volatile Chemical Precursors, Sub-Contract by ManTech Environmental Technology, Inc.

to Contract No. F08635-93-C-0020 for the Armstrong Laboratory Environics Directorate, Tyndall AFB, FL, 1996). Rate constants were measured, using a relative rate method with gas chromatographic analysis, for the reactions of OH radicals with $(CH_3O)_2P(O)CH_3$, $(C_2H_5O)_2P(O)CH_3$ and $(CH_3O)_2P(O)H$, with rate constants (in units of 10^{-12} cm^3 molecule^{-1} s^{-1}) of 6.32 ± 0.29, 32.2 ± 1.1, and 4.94 ± 0.19, respectively. The rate constant of Kleindienst and Smith for reaction of OH radicals with $(CH_3O)_2P(O)H$, $(4.94 \pm 0.19) \times 10^{-12}$ cm^3 molecule^{-1} s^{-1}, is in excellent agreement with the value measured here of $(5.08 \pm 0.53) \times 10^{-12}$ cm^3 molecule^{-1} s^{-1}.

Acknowledgment. This work was supported by funds from the Pacific Northwest National Laboratory (Contract No. 283369-A-G2). P. Martin gratefully acknowledges financial support from the Spanish Ministerio de Educacion y Cultura.

References and Notes

(1) Toy, A. D. F.; Walsh, E. N. *Phosphorus Chemistry in Everyday Living*; American Chemical Society, Washington, DC, 1987; pp 135−163 and 219−253.

(2) Atkinson, R. *Atmos. Environ.* **2000**, *34*, 2063.

(3) Fritz, B.; Lorenz, K.; Steinert, W.; Zellner, R. Laboratory Kinetic Investigations of the Tropospheric Oxidation of Selected Industrial Emissions. In *Physico-Chemical Behavior of Atmospheric Pollutants*, Proceedings of the Second European Symposium, Varese, Italy, 29 Sep.−1 Oct. 1981; Versino, B., Ott, H., Eds.; D. Reidel Publishing Co.: Dordrecht, The Netherlands, 1982; pp 192−202.

(4) Jourdain, J. L.; Le Bras, G.; Combourieu, J. *J. Phys. Chem.* **1982**, *86*, 4170.

(5) Jourdain, J. L.; Laverdet, G.; Le Bras, G.; Combourieu, J. *J. Chim. Phys.* **1980**, *77*, 809.

(6) Tuazon, E. C.; Atkinson, R.; Aschmann, S. M.; Arey, J.; Winer, A. M.; Pitts, J. N., Jr. *Environ. Sci. Technol.* **1986**, *20*, 1043.

(7) Atkinson, R.; Aschmann, S. M.; Goodman, M. A.; Winer, A. M. *Int. J. Chem. Kinet.* **1988**, *20*, 273.

(8) Goodman, M. A.; Aschmann, S. M.; Atkinson, R.; Winer, A. M. *Arch. Environ. Contam. Toxicol.* **1988**, *17*, 281.

(9) Goodman, M. A.; Aschmann, S. M.; Atkinson, R.; Winer, A. M. *Environ. Sci. Technol.* **1988**, *22*, 578

(10) Atkinson, R.; Carter, W. P. L.; Winer, A. M.; Pitts, J. N., Jr. *J. Air Pollut. Control Assoc.* **1981**, *31*, 1090.

(11) Tuazon, E. C.; Carter, W. P. L.; Atkinson, R.; Pitts, J. N., Jr. *Int. J. Chem. Kinet.* **1983**, *15*, 619.

(12) Tuazon, E. C.; Aschmann, S. M.; Atkinson, R. *Environ. Sci. Technol.* **2000**, *34*, 1970.

(13) Aschmann, S. M.; Martin, P.; Tuazon, E. C.; Arey, J.; Atkinson, R. *Environ. Sci. Technol.* **2001**, *35*, 4080.

(14) Aschmann, S. M.; Chew, A. A.; Arey, J.; Atkinson, R. *J. Phys. Chem. A* **1997**, *101*, 8042.

(15) Taylor, W. D.; Allston, T. D.; Moscato, M. J.; Fazekas, G. B.; Kozlowski, R.; Takacs, G. A. *Int. J. Chem. Kinet.* **1980**, *12*, 231.

(16) DeMore, W. B.; Sander, S. P.; Golden, D. M.; Hampson, R. F.; Kurylo, M. J.; Howard, C. J.; Ravishankara, A. R.; Kolb, C. E.; Molina, M. J. *Chemical Kinetics and Photochemical Data for Use in Stratospheric Modeling*; Jet Propulsion Laboratory Publication 97-4, Pasadena, CA, January 15, 1997; Evaluation 12, p 142.

(17) Prinn, R. G.; Weiss, R. F.; Miller, B. R.; Huang, J.; Alyea, F. N.; Cunnold, D. M.; Fraser, P. J.; Hartley, D. E.; Simmonds, P. G. *Science* **1995**, *269*, 187.

(18) Hein, R.; Crutzen, P. J.; Heimann, M. *Global Biogeochem. Cycles* **1997**, *11*, 43.

(19) Atkinson, R.; Baulch, D. L.; Cox, R. A.; Hampson, R. F., Jr.; Kerr, J. A.; Rossi, M. J.; Troe, J. *J. Phys. Chem. Ref. Data* **1999**, *28*, 191.

(20) Kramp, F.; Paulson, S. E. *J. Phys. Chem. A* **1998**, *102*, 2685.

(21) Atkinson, R. *J. Phys. Chem. Ref. Data* **1994**, *Monograph 2*, 1.

(22) Atkinson, R. *J. Phys. Chem. Ref. Data* **1997**, *26*, 215.

(23) Neidlein, R.; Buseck, S. *Helv. Chim. Acta* **1992**, *75*, 2520.

(24) Bibout, M. E. M.; Hannioui, A.; Peiffer, G.; Samat, A.; Pannell, K. H. *Synth. Commun.* **1993**, *23*, 2273.

(25) Atkinson, R.; Aschmann, S. M.; Carter, W. P. L.; Winer, A. M.; Pitts, J. N., Jr. *J. Phys. Chem.* **1982**, *86*, 4563.

(26) Pouchert, C. J. *The Aldrich Library of Infrared Spectra*, 2nd ed.; Milwaukee, WI, 1975; pp 483−495.

(27) Pouchert, C. J. *The Aldrich Library of FT-IR Spectra*, 1st ed.; Milwaukee, WI, 1989; Vol. 3, pp 837−847.

(28) Plumb, J. B.; Griffin, C. E. *J. Org. Chem.* **1963**, *28*, 2908.

(29) Thompson, Q. E. *J. Am. Chem. Soc.* **1961**, *83*, 845.

(30) *Standard Ultraviolet Spectra Collection*; Sadtler Laboratories: Philadelphia, 1975−1995. See, for example, Nos. 5865 and 28867.

(31) Ma, S.; Barnes, I.; Becker, K. H. *Environ. Sci. Technol.* **1998**, *32*, 3515.